PROCEEDINGS OF SCIENCE

Understanding the origin of the break in the cosmic-ray all-electron spectrum at around 1 TeV

Satyendra Thoudam[a,*]

[a] *Department of Physics, Khalifa University of Science and Technology, P.O. Box 127788, Abu Dhabi, United Arab Emirates*

E-mail: satyendra.thoudam@ku.ac.ae

Measurements of the cosmic-ray electrons plus positrons by several experiments such as CALET, DAMPE and H.E.S.S. have revealed the presence of a spectral break at around 1 TeV whose origin is still unclear. In this contribution, we explore different possibilities for the origin which include an electron source spectrum with a broken power law which is expected from the radiative cooling of electrons during their confinement inside supernova remnants, a power law with an exponential or super-exponential cut-off as expected when the maximum energy of the electrons is limited either by free escape from the acceleration region or by radiative losses (or by the finite age of the accelerator) respectively, and a scenario with the absence of nearby potential sources. We will show that the broken power-law source spectrum best explains the observed data, and we will discuss the implications of the result on the nature of cosmic-ray escape from the source region into the Galaxy.

39th International Cosmic Ray Conference (ICRC2025)
15–24 July 2025
Geneva, Switzerland

*Speaker

PoS(ICRC2025)142

1. Introduction

Recent measurements of cosmic-ray (CR) electrons plus positrons spectrum by the AMS-02 [1], CALET [2], DAMPE [3], and H.E.S.S. [4, 5] experiments have revealed puzzling spectral structures which are difficult to explain under the standard model of CR acceleration and propagation in the Galaxy. One prominent feature is a sharp break at $\sim$ 1 TeV with the spectrum following $\sim E^{-3}$ below the break and $\sim E^{-4}$ above the break up to about 10 TeV. The origin of the break is not clearly understood. It is difficult to explain as an effect of the propagation of CRs in the Galaxy. High-energy electrons undergoing diffusive propagation in the Galaxy suffer radiative losses which results into an equilibrium spectrum that is steeper than their injected source spectrum as $E^{-(\Gamma+1-\xi)}$, where Γ is the source index and $\xi = (1-a)/2$ is a correction factor which depends on the index of the diffusion coefficient, $D(E) \propto E^a$. The value of ξ is $\sim (0.2 - 0.35)$ for the typical range of $a \sim (0.3 - 0.6)$ adopted in most common models of CR propagation in the Galaxy. The equilibrium spectrum is expected to follow a continuous power-law without any break in energy in contrast to the observed spectrum. It is also unlikely that the observed break is caused by the suppression in the positron flux at high energies. The positron flux shows a continuous decrease above $\sim$ (300 – 400) GeV, contributing only about 10% of the combined electron plus positron flux at $\sim$ 1 TeV [23]. All these suggest that the observed break most likely have an origin related to the source properties of CR electrons, such as the absence of nearby sources and a cutoff (exponential or super-exponential) or a power-law break in the source spectrum. All these scenarios are investigated, and show that the broken power-law scenario best reproduces the observed break at $\sim$ 1 TeV and the overall electron plus positron spectrum at the same time, as discussed in Ref. [7].

2. Propagation of CR electrons in the Galaxy

The diffusive propagation of high-energy CR electrons in the Galaxy subject to radiative losses is described by,

$$\nabla \cdot (D\nabla N) + \frac{\partial}{\partial E}\{b(E)N\} = -q, \tag{1}$$

where E is the kinetic energy of the electron, $N(\mathbf{r}, E)$ is the number density at a position $\mathbf{r} \equiv (r, \phi, z)$ in cylindrical coordinates with the origin located at the position of the Sun, and $q(\mathbf{r}, E)$ is the source term which denotes the injection rate of CR electrons per unit volume into the interstellar medium (ISM). Following Ref. [8], we take the diffusion coefficient as $D(E) = D_0\beta(E/E_0)^a$, where $D_0 = 1.55 \times 10^{28}$ cm^2 s^{-1}, $\beta = v/c$ is the ratio of the particle velocity v to the velocity of light c, $E_0 = 3$ GeV, and $a = 0.54$ is the diffusion index. The radiative energy loss rate, $b(E)$, due to synchrotron and inverse Compton losses is taken as [9],

$$b(E) = \frac{4}{3}\sigma_{\rm T} c \left(\frac{E}{m_{\rm e}c^2}\right)^2 \left[U_{\rm B} + \sum_{i=1}^{4} \frac{W_{\rm i} E_{\rm i}^2}{E^2 + E_{\rm i}^2}\right], \tag{2}$$

where $\sigma_{\rm T}$ is the Thomson cross-section, $m_{\rm e}c^2$ the electron rest-mass energy, and $U_{\rm B} = B^2/8\pi$ the magnetic field energy density in which we take $B = 3\,\mu$G which represents the average magnetic field over the $z = \pm 5$ kpc region below and above the Galactic plane at the galactocentric radius of 8.5 kpc. This value of B is calculated using $B(z) = B_0\, e^{-|z|/3{\rm kpc}}\,\mu$G adopted in the GALPROP CR

propagation code [10], using the local magnetic field value of $B_0 = 6\,\mu$G [11]. The inverse Compton losses is considered in the Klein-Nishina limit with four different photon background fields in the ISM. The energy density W_i and the critical Klein-Nishina energy E_i of these photon fields are taken as $(0.09\ \mathrm{eV/cm^3}, 40\ \mathrm{GeV})$ for photons from spectral type B stars, $(0.3\ \mathrm{eV/cm^3}, 161\ \mathrm{GeV})$ for photons from spectral type G-K stars, $(0.4\ \mathrm{eV/cm^3}, 4.0\times10^4\ \mathrm{GeV})$ for infrared radiation, and $(0.25\ \mathrm{eV/cm^3}, 3.0\times10^5\ \mathrm{GeV})$ for cosmic microwave background [9].

The Green's function solution of Eq. (1) is given by,

$$G(\mathbf{r},\mathbf{r}',E,E') = \frac{1}{8\pi^{3/2}b(E)A^{3/2}}\exp\left(-\frac{(\mathbf{r}-\mathbf{r}')^2}{4A}\right) \tag{3}$$

where $A(E,E') = \int_E^{E'}\frac{D(u)}{b(u)}du$. For sources uniformly distributed in r and ϕ in the Galactic disk, the source term is written as $q(\mathbf{r},E) = \nu Q(E)\delta(z)$, where $\nu = 25\ \mathrm{Myr^{-1}\ kpc^{-2}}$ represents the rate of supernova explosions per unit surface area in the disk [12], and $Q(E)$ is the source spectrum. Using Eq. 3, the CR electron density at the Earth ($\mathbf{r} = 0$) due to all the sources located beyond r_0, is obtained as,

$$\begin{aligned} N(E) &= 2\pi\nu\int_E^\infty dE'\int_{r_0}^\infty r'dr'\int_{-\infty}^\infty dz' G(r',z',E,E')Q(E')\delta(z') \\ &= \frac{\nu}{\sqrt{\pi}b(E)}\int_E^\infty \frac{Q(E')}{r_\mathrm{d}}\exp\left(-\frac{r_0^2}{r_\mathrm{d}^2}\right)dE'. \end{aligned} \tag{4}$$

where we have written $r_\mathrm{d}(E,E') = 2\sqrt{A(E,E')}$ which represents the average diffusion length of an electron of energy E' before it cools down to energy E. For an electron of 1 TeV, the diffusion length before losing half its energy is $r_\mathrm{d} \sim 1.16$ kpc for the values of the diffusion coefficient and the magnetic field strength considered in the present study. In general, r_d decreases as a function of energy as $r_\mathrm{d} \propto E^{(a-1)/2}$. For the value of $a = 0.54$ considered in this work, $r_\mathrm{d} \propto E^{-0.23}$ [7].

The electron flux at the Earth from a continuous distribution of sources throughout the Galactic disk is obtained from Eq. (4) by setting $r_0 = 0$ as,

$$N(E) = \frac{\nu}{\sqrt{\pi}b(E)}\int_E^\infty \frac{Q(E')}{r_\mathrm{d}}dE'. \tag{5}$$

For $Q(E) \propto E^{-\Gamma}$, $D(E) \propto E^a$ and $b(E) \propto E^2$, one can check from Eq. (5) that the spectrum at the Earth follows $N(E) \propto E^{-\Gamma-1+\xi}$. The spectrum gets modified mainly due to the radiative losses, but with a small correction factor $\xi = (1-a)/2$ resulting from the diffusive propagation. For $a = 0.54$, we get $\xi = 0.23$.

3. Different scenarios for the spectral break

Missing sources: High energy CR electrons cannot travel far distances in the Galaxy due to significant radiative losses they suffer during their propagation. Therefore, if nearby CR sources are missing, it can lead to a flux suppression at high energies [13]. In order to produce a suppression above $\sim$ 1 TeV, the nearest source must be located around 1 kpc from the Earth. The shape of the spectral break in this scenario is given by the exponential term, $\exp\left(-r_0^2/r_\mathrm{d}^2\right)$, in Eq. (4).

Defining r_0 as the diffusion length of electrons corresponding to the break energy E_0, we can write $r_0 \propto E_0^{(a-1)/2}$ which gives $r_0 \propto E_0^{-0.23}$ for $a = 0.54$. Recalling $r_\mathrm{d} \propto E^{-0.23}$ obtained in Section 2, the exponential term in Eq. (4) becomes $\exp\left[-(E/E_0)^{0.46}\right]$, which is close to $\exp\left(-\sqrt{E/E_0}\right)$.

Exponential cut-off: Under the diffusive shock acceleration theory, it has been predicted that if the maximum energy of the particles is limited by the free escape boundary of the acceleration region, the spectrum can follow an exponential cutoff of the form $\exp(-E/E_0)$ ([14, 15] and references therein). Such a spectral cut-off is most commonly used in CR propagation studies (e.g., [13, 16]). In the test particle approximation, the spectrum at the shock in this case follows $f_0(E) \propto \exp\left[-q\,(E/E_\mathrm{m})^{\beta}\right]$, where $q = 3r/(r-1)$, with the shock compression ratio $r = 4$ for strong shocks, and E_m is the maximum energy of the particles that remain confined [14, 15]. For Bohm diffusion, $\beta = 1$, which gives a cutoff shape that follows $\exp(-E/E_0)$, where we have written $E_0 = E_\mathrm{m}/q$.

Super-exponential cut-off: In situations where the the maximum energy of the electrons in the diffusive shock acceleration process is limited by radiative losses or by the finite age of the accelerator, the spectrum is predicted to follow a super-exponential cutoff $\exp\left[-(E/E_0)^2\right]$ [17–19]. The electron spectrum at the shock front at very high energies where the radiative energy loss dominates over the energy gain from acceleration is given as $f_0(E) \propto \exp\left[-q\,(E/E_\mathrm{m})^{\beta+1}\right]$ [17]. Then, for Bohm-like diffusion, the spectral cut-off follows $\exp\left[-(E/E_0)^2\right]$, where $E_0 = E_\mathrm{m}/\sqrt{q}$.

Broken power-law: In the standard theory of diffusive shock acceleration applied to supernova remnant (SNR) shocks, after acceleration, majority of the particles escape downstream of the shock and remain confined within the remnant until the shock slows down. High-energy electrons can suffer radiative losses during the confinement, and this can lead a power-law break in the electron spectrum at high energy [20–22]. The position of the break depends on the age of the remnant. The electron spectrum during the confinement in this scenario is found to follow $f(E,t) \propto E^{-\Gamma}$ for $E < E_0$ and $f(E,t) \propto E^{-(\Gamma+1)}$ for $E \geq E_0$, where Γ is the spectral index of electrons accelerated at the shock and $E_0 \propto 1/t$ is the break energy whose value decreases with the age t of the remnant. It is assumed that all the particles get released into the ISM when the shock slows down significantly and can no longer effectively confine the particles.

4. Fitting procedure of the observed spectrum

Following the description of the different scenarios in Section 3, we consider different forms of the source spectrum $Q(E)$ for the calculation of the CR electron spectrum:

$$
\begin{aligned}
Q(E) &= kE^{-\Gamma}, \text{ Missing sources} \\
&= kE^{-\Gamma}\exp\left(-\frac{E}{E_0}\right), \text{ Exponential cutoff} \\
&= kE^{-\Gamma}\exp\left(-\frac{E^2}{E_0^2}\right), \text{ Super exponential cutoff} \\
&= kE^{-\Gamma}\left[1+\left(\frac{E}{E_0}\right)^{1/\delta}\right]^{-\delta}, \text{ Broken power law,}
\end{aligned}
\tag{6}
$$

where k is a constant that depends on the fraction f of the supernova kinetic energy of 10^{51} ergs injected into CR electrons, Γ is the source index, and E_0 represents either the exponential cut-off, super-exponential cut-off or the power-law break energy. For the broken power-law, Equation 6 reproduces a spectrum that follows $E^{-\Gamma}$ and $E^{-(\Gamma+1)}$ below and above E_0 respectively, as discussed in Section 3. The smoothness parameter δ is fixed at 0.05. Using $Q(E)$ from Equation 6, the electron spectrum for the missing source scenario is calculated using Equation 4 by keeping r_0 as a model parameter, and for the other scenarios, Equation 5 is used.

The fits are performed using three free parameters for each scenario: (f, Γ, r_0) for the missing sources and (f, Γ, E_0) for the other cases. We marginalize f to determine the best-fit values of (Γ, r_0) or (Γ, E_0) that gives the maximum likelihood, $\mathcal{L} = \sum_f \mathcal{L}_f$, where $\mathcal{L}_f = \exp\left(-\chi^2/2\right)$ and

$$\chi^2 = \sum_i \frac{[I_{\rm D}(E_{\rm i}) - I_{\rm M}(E_{\rm i})]^2}{\sigma_{\rm D}^2(E_{\rm i})} + \sum_i \frac{[I_{\rm H}(E_{\rm i}) - I_{\rm M}(E_{\rm i})]^2}{\sigma_{\rm H}^2(E_{\rm i})}. \tag{7}$$

The summations in Equation 7 are performed over the measured energy points $E_{\rm i}$, and $(I_{\rm D}, \sigma_{\rm D})$, $(I_{\rm H}, \sigma_{\rm H})$ represents the measured electron plus positron flux and the associated errors from the DAMPE and the H.E.S.S. experiments, respectively. The model flux $I_{\rm M}(E_{\rm i}) = I_{\rm e^-}(E_{\rm i}) + I_{\rm e^+}(E_{\rm i})$, where $I_{\rm e^-}(E_{\rm i}) = (v/4\pi)N(E_{\rm i})$ is the predicted electron flux by our model (Equations 4 or 5), and $I_{\rm e^+}(E_{\rm i})$ is the measured positron flux from the AMS-02 experiment described as [23],

$$I_{e^+}(E_{\rm i}) = \frac{E_{\rm i}^2}{\hat{E}^2}\left[K_1\left(\frac{\hat{E}}{E_1}\right)^{\gamma_1} + K_2\left(\frac{\hat{E}}{E_2}\right)^{\gamma_2}\exp\left(-\frac{\hat{E}}{E_{\rm c}}\right)\right]. \tag{8}$$

In Equation 8, $\hat{E} = E_{\rm i} + \phi$, with $\phi = 1.1$ GeV is the solar modulation parameter, $K_1 = 6.51 \times 10^{-2}$ $(\mathrm{m^2\,sr\,s\,GeV})^{-1}$, $K_2 = 6.80 \times 10^{-5}$ $(\mathrm{m^2\,sr\,s\,GeV})^{-1}$, $E_1 = 7.0$ GeV, $E_2 = 60$ GeV, $\gamma_1 = -4.07$, $\gamma_2 = -2.58$, and $E_{\rm c} \approx 813$ GeV [23]. Once the best-fit values of (Γ, r_0) or (Γ, E_0) are determined, we scan over f to determine its best-fit value that gives the minimum χ^2 value.

The fitting procedure described above is performed for the energy range of (20 − 3500) GeV. This excludes the three highest energy measured data points shown in Figure 1. At these energies, the contamination from one or more nearby strong discrete sources can be significant which might produce a rising trend in the flux as studied in Ref. [13]. Such as effect is not included in the present study.

5. Results and discussion

The best-fit electron plus positron spectra are shown in Figure 1 (top panel) for the different scenarios – missing sources (green line), exponential cut-off (black line), super-exponential cut-off (blue line), and broken power-law (thick red line) – along with the all-electron (electron plus positron) spectra measured by the DAMPE and the H.E.S.S experiments. The positron spectrum (thin red line) given by Equation 8 and its data are from the AMS-02 experiment. The fits are performed for the (20 − 3500) GeV range. All the scenarios predict similar spectra up to energies close to $\sim$ 1 TeV, while above this energy, their predictions start to differ with the broken power-law and the super-exponential cut-off scenarios explaining the data better than the missing sources and the exponential cut-off scenarios. The residuals of the fits are shown in the bottom panel which is

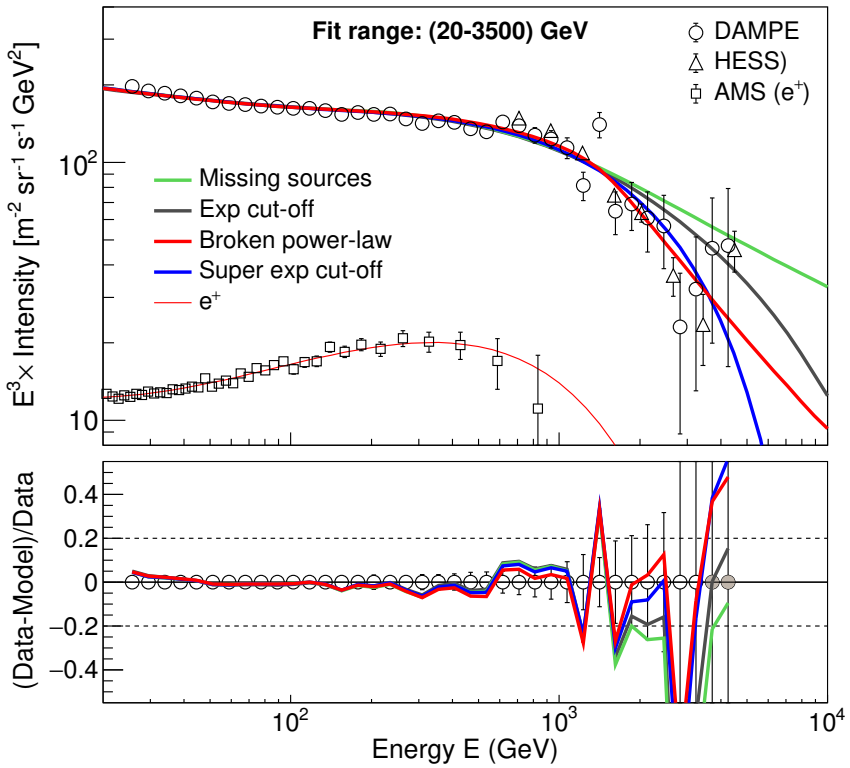

Figure 1: Top panel: Best-fit all-electron (electron plus positron) spectra for the different scenarios of the spectral break – missing sources (green line), exponential cutoff (black line), broken power-law (thick red line), and super-exponential cutoff (blue line). The fits are performed for the (20 − 3500) GeV range. The all-electron data are from DAMPE [3] and H.E.S.S. [4] experiments, and the positron data are from AMS-02 experiment [23]. The thin red line represents the positron spectrum given by Equation 8. Bottom panel: Residuals of the fits, shown only with respect to the DAMPE data although the χ^2 calculation includes both the DAMPE and the H.E.S.S. data. The filled circles in the residual plot represent the points not included in the fit. The dashed horizontal lines represent the ±20% residual levels, shown only for reference. The best-fit values of the model parameters and the χ^2 are listed in Table 1. Figure adapted from Ref. [7].

calculated only with respect to the DAMPE data, although both DAMPE and H.E.S.S data were included in the fits. The dashed lines show the ±20% residual levels, and the filled circles in the residual plot represent the data points which were not included in the fits. The best-fit values of the different parameters, (f, Γ, r_0) for the missing sources scenario and (f, Γ, E_0) for the other cases, are listed in Table 1 along with the χ^2 values of the fits. Looking at the χ^2 values, the broken power-law scenario gives the best result of all the scenarios with the smallest χ^2 value of 69. The next best scenario is the super-exponential cut-off with $\chi^2 = 87$. The exponential cut-off and the missing sources scenarios give $\chi^2 = 114$ and 125, respectively.

The broken power-law scenario gives best-fit values of $\Gamma = 2.39$, $E_0 = 1576$ GeV, and $f = 0.159 \times 10^{49}$ ergs. Simulation of DSA applied to supernova shocks also predicts a similar break in the power-law spectrum of electrons at GeV−TeV range [21]. It may be noted that our best-fit value pf $\Gamma = 2.39$ is larger than the typical value of 2.0 predicted by the standard theory of DSA for strong shocks. This difference might indicate some level of spectral modification

Table 1: Best-fit values of the model parameters (f, Γ, E_0, r_0) and the χ^2 values of the fits for the different scenarios of the spectral break. The fit is performed for the (20 – 3500) GeV range.

Scenario type	f ($\times 10^{49}$ ergs)	Γ	E_0 (GeV)	r_0 (kpc)	χ^2 (ndf = 43)
Missing sources	0.272	2.23	–	0.85	125
Exponential cutoff	0.154	2.37	6762	–	114
Super-exponential cutoff	0.159	2.39	4588	–	87
Broken power-law	0.159	2.39	1576	–	69

(steepening) happening during the escape of CRs from the source region. Recent studies have shown that CR protons while escaping can generate magnetic fluctuations around the source region, due to resonant and non-resonant streaming instabilities [24]. These fluctuations can produce a low-diffusivity bubbles surrounding the sources where CRs spend a considerable time before finally escaping into the ISM. For electrons, it is quite possible that radiative losses modify their spectrum while they diffuse through these bubbles.

A strong observation evidence in favour of the broken power-law scenario is provided by the observations of non-thermal radiation from SNRs. Multi-wavelength study of the SNR RX J1713.7 – 3946 using X-ray to TeV gamma-ray data has found preference for a broken power-law electron spectrum with a break energy at $E_{\rm b}$ = 2.5 TeV, an index Γ = 1.78 (2.93) below (above) the break and an exponential cut-off of $E_{\rm c} \sim$ 88 TeV for a magnetic field strength of $\sim$ 14 μG [25]. The Γ value obtained below the break is smaller than our best-fit value of Γ = 2.39, but what is striking is that the spectral difference of $\Delta\Gamma \sim$ 1.15 found below and above the break is quite close to our prediction of $\Delta\Gamma \sim$ 1.0 by the broken power-law scenario. Additional evidence for the broken power-law scenario comes from the multi-wavelength studies of several other SNRs [26]. Based on a sample of seven middle-aged (few thousand years old) shell-type SNRs, they found that the majority of the SNRs show an electron spectrum with a power-law break at $E_{\rm b} \sim$ (1.0 – 3.5) TeV, $\Gamma \sim$ 1.9 – 2.2 below the break, a high-energy super-exponential cutoff in the range of $\sim$ (30 – 80) TeV and a magnetic field of $B \sim$ (9 – 26) μG. The fact that these Γ values are close to the value predicted by the DSA theory indicates that the electrons confined inside the remnants mostly preserve the shape of the spectrum produced at the shocks.

6. Conclusion

We have explored different scenarios for the origin of the observed break in the all-electron spectrum at $\sim$ 1 TeV, and find that the broken power-law scenario best describes the data. Based on our best-fit results and evidence from the multi-wavelength studies of SNRs, we conclude that if SNRs are the main sources of CRs in the Galaxy, the observed spectral break is most likely an imprint of radiative cooling break in the electron source spectrum. Our study further shows that CR electrons must undergo spectral modifications while escaping the source region in order to

reconcile the difference in the source index required for CR propagation study and that obtained from the study of SNRs.

References

[1] Aguilar, M. et al. 2019a, PRL, 122, 101101

[2] Adriani, O. et al. 2017, PRL, 119, 181101

[3] Ambrosi, G. et al. 2017, Nature, 552, 63

[4] Aharonian, F. A. et al. 2008, PRL, 101, 261104

[5] Aharonian, F. A. et al. 2024, PRL, 133, 221001

[23] Aguilar, M. et al. 2019b, PRL, 122, 041102

[7] Thoudam, S., 2024, A&A, 690, A351

[8] Thoudam, S., & Hörandel, J.R. 2013, MNRAS, 435, 2532

[9] Schlickeiser, R. & Ruppel, J. 2010, New J. Phys., 12, 033044

[10] Strong, A. W. et al., 2010, ApJL, 722, L58

[11] Beck, R., 2001, Space Science Reviews, 99, 243

[12] Grenier I. A., 2000, A&A, 364, L93

[13] Kobayashi, T., Komori, Y., Yoshida, K. & Nishimura, J., 2004, ApJ, 601, 340

[14] Caprioli, D., Blasi, P., & Amato, E. 2009, MNRAS, 396, 2065

[15] Ohira, Y., Murase, K., & Yamazaki, R. 2010, A&A, 513, A17

[16] Thoudam, S., et al. 2016, A&A, 595, A33

[17] Zirakashvili, V.N. & Aharonian, F.A., 2007, A&A, 465, 695

[18] Kang, H., Ryu, D., & Jones, T. W., 2009, ApJ, 695, 1273

[19] Blasi, P., 2010, MNRAS, 402, 2807

[20] Thoudam, S., & Hörandel, J.R. 2011, MNRAS, 414, 1432

[21] Kang, H., 2011, JKAS, 44, 49

[22] Ohira, Y., & Yamazaki, R. 2017, JHEAp, 13, 17

[23] Aguilar, M. et al. 2019b, PRL, 122, 041102

[24] Schroer, B., Pezzi, O., Caprioli, D., Haggerty, C., & Blasi, P. 2021, ApJL, 914, L13

[25] Abdalla, H., et al. 2018, A&A 612, A6

[26] Zang, X., & Liu, S. 2019, ApJ, 876, 24